Inorg. Chem. **2009**, *48*, 455−465

Pyridine-*N*-oxide Analogues of DOTA and Their Gadolinium(III) Complexes Endowed with a Fast Water Exchange on the Square-Antiprismatic Isomer†

Miloslav Polášek,‡ Miroslava Šedinová,‡ Jan Kotek,‡ Luce Vander Elst,§ Robert N. Muller,§ Petr Hermann,*,‡ and Ivan Lukeš‡

Department of Inorganic Chemistry, Charles University, Hlavova 2030, 128 40 Prague 2, Czech Republic, and NMR and Molecular Imaging Laboratory, Department of General, Organic and Biomedical Chemistry, University of Mons-Hainaut, Avenue du champ de Mars 24, B-7000 Mons, Belgium

Received August 21, 2008

Two macrocyclic ligands derived from H_4dota containing three acetate pendant arms and one 2-methylpyridine-*N*-oxide coordinating unit were synthesized. The ligand H_3do3apy^{NO} (H_3**L**^{1}, 10-[(1-oxidopyridin-2-yl)methyl]-1,4,7,10-tetraazacyclododecane-1,4,7-triacetic acid) contains an unsubstituted pyridine-*N*-oxide ring; the ligand H_4do3apy$^{NO\text{-}C}$ (H_4**L**^{2}, 10-[(4-carboxy-1-oxidopyridin-2-yl)methyl]-1,4,7,10-tetraazacyclododecane-1,4,7-triacetic acid) is functionalized with a carboxylic group in the 4 position of the pyridine ring to allow attachment to other molecules. The ligands form octadentate (N_4O_4 environment) Ln^{III} complexes, with one water molecule completing the coordination sphere in a capping position. The complexes are present in solution exclusively as square-antiprismatic isomers over the whole lanthanide series. The introduction of the carboxylic group to the pyridine-*N*-oxide unit in H_4**L**^{2} has no significant effect on the hydration number ($q = 1$) and the water exchange rate of the [Gd(H_2O)(**L**$_2$)]$^-$ complex compared to the parent [Gd(H_2O)(**L**^{1})] complex (water residence times: $\tau_M = 39$ ns for [Gd(H_2O)(**L**^{1})] and $\tau_M = 34$ ns for [Gd(H_2O)(**L**^{2})]$^-$ at 298 K).

Introduction

Magnetic resonance imaging (MRI) is one of today's most important diagnostic methods, and it is particularly indispensable for imaging of soft tissues rich in water content. The basic MRI image reflects the concentration of protons because the signal of ^{1}H nuclei is usually observed. In addition, the longitudinal (T_1) and transversal (T_2) relaxation times of the protons can also be used to further improve the image if the content of water in the examined tissue is quite homogeneous. The relaxation times can be shortened by the administration of paramagnetic contrast agents (CAs), which serve as catalysts for the relaxation processes. A very potent substance for the T_1 shortening is the highly paramagnetic Gd^{III} ion. However, this ion must be bound in very stable complexes with polydentate ligands to preclude the release of the toxic Gd^{III} aqua ion. Typical examples of the appropriate chelators are the macrocyclic DOTA or acyclic DTPA (Chart 1). Though being successfully clinically used for many years, the complexes of DOTA and DTPA show only a low efficiency and demand a high dosage to give the desired effect. The efficiency of the CA is represented by its relaxivity (r_1), i.e., the relaxation rate enhancement of water protons in a 1 mM solution of the CA. Typical relaxivities of current commercial CAs are in the range of 4−5 s^{-1} mM^{-1} for a magnetic field of 0.47 T (i.e., proton Larmor frequency of 20 MHz), while the theoretical upper limit is about 100 s^{-1} mM^{-1}.

Some parameters closely associated with the function of the T_1-CA have been recognized to play a major role in the final relaxivity.[2−5] In principle, the magnetic information carried by the CA has to be transferred from unpaired electrons of the Gd^{III} ion to protons of bulk water molecules. This occurs mainly through mediation of the water molecule(s) coordinated to the central ion, which is exchanged

† Dedicated to Dr. Joop A. Peters (Delft University of Technology, Delft, The Netherlands) on the occasion of his 65th birthday in appreciation of his contribution in the field of NMR investigation of lanthanide complexes.

* To whom correspondence should be addressed. E-mail: petrh@natur.cuni.cz. Tel: (+420)22195-1263. Fax: (+420)22195-1253.

‡ Charles University.

§ University of Mons-Hainaut.

10.1021/ic801596v CCC: $40.75
Published on Web 12/17/2008

Chart 1. Structures of Ligands Discussed in This Work

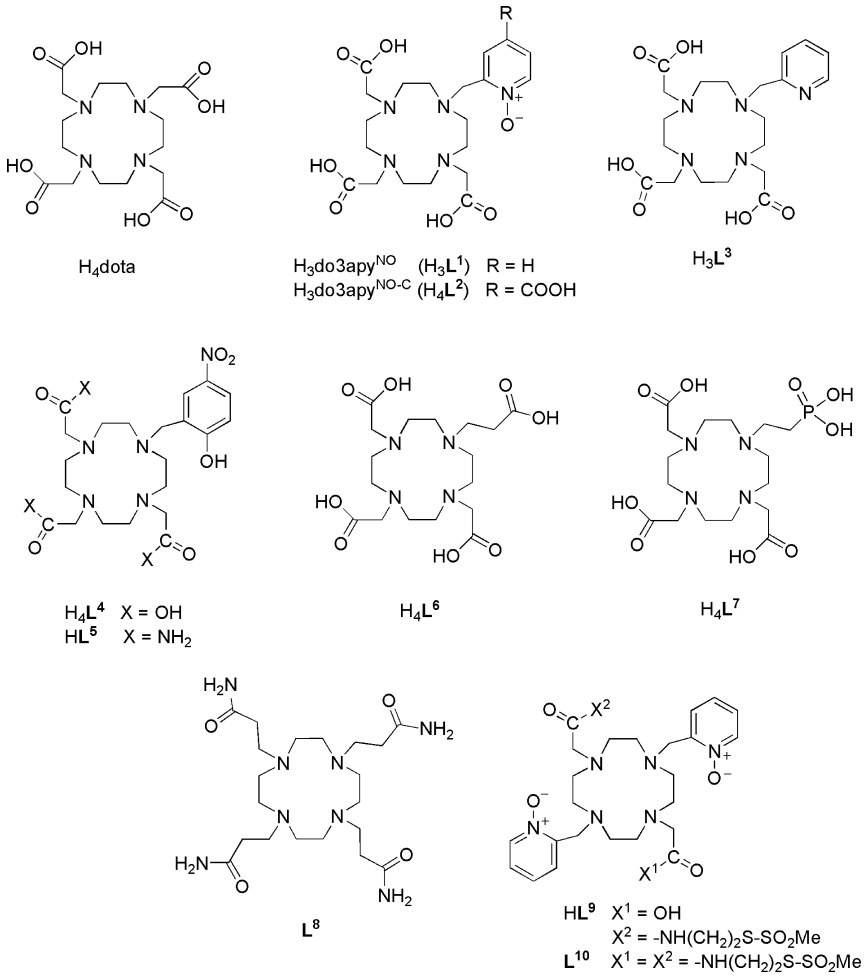

with the bulk molecules with a certain rate (k_{ex}). In addition, an effective transfer of the information is influenced by a reorientation of the Gd−H vector in the magnetic field, i.e., by tumbling of the molecule. Finally, the relaxivity is affected by relaxation of the unpaired electrons of the central ion. The crucial parameters determining the relaxivity of the complex are thus the number of coordinated water molecules (q), their mean residential time in the first coordination sphere ($\tau_M = 1/k_{ex}$), the rotational correlation time (τ_R), and the electronic parameters of the Gd^{III} ion (τ_v and Δ^2). These parameters also represent a weak point of the clinically used CAs. In most cases, q is equal to 1, but higher values would be more advantageous. The slow water exchange rate and fast molecular motion (represented by the short τ_R) impose other limitations. Fortunately, optimization of these parameters is possible by careful structural modification of the ligand molecule.[4,5] Attempts to increase q to values higher than 1 have mostly led to a lower stability of the complexes and hence increased toxicity.[5] Thus, the complexes with $q = 1$ are most suitable for further development. Nonetheless, successful ways of optimizing τ_M and τ_R were found.[4−6] For example, an increased steric strain around the water binding site accelerates the water exchange because it facilitates the dissociative exchange mechanism.[2,5] Such an effect can be achieved, for instance, by increasing the number of atoms in one of the chelate rings from the usual five to six or more atoms in the complexes with both open-chain[7,8] or macrocyclic[8−10] ligands. Methods of increasing τ_R rely on conjugation of the low-molecular-weight complexes to slowly rotating macromolecules through either covalent[5,11,12] or noncovalent bonding interactions.[4,13] However, the effect may be hampered by an internal flexibility of the macromolecular scaffold and/or the linker.[5,14−16] Moreover, the conjugation may result in a change of τ_M if the attachment point is situated in close proximity to the metal center. For instance, this happens when a chelating carboxylate group is utilized for conjugation and is turned into an amide, leading to an elongation of the water residential time.[2,5,14,17] Such effects make the simultaneous adjustment of τ_M and τ_R difficult.

In this work, we report on detailed syntheses of two derivatives of DOTA bearing the pyridine-*N*-oxide pendant

(1) Aime, S.; Botta, M.; Fasano, M.; Terreno, E. *Chem. Soc. Rev.* **1998**, *27*, 19–29.
(2) Merbach, A. E.; Tóth, É. *The Chemistry of Contrast Agents in Medical Magnetic Resonance Imaging*; John Wiley & Sons: Chichester, U.K., 2001.
(3) Krause, W. Contrast agents I. Magnetic resonance imaging. *Topics in Current Chemistry*; Springer Verlag:: Heidelberg, 2002; Vol. *221*.
(4) Caravan, P. *Chem. Soc. Rev.* **2006**, *35*, 512–523.
(5) Hermann, P.; Kotek, J.; Kubíček, V.; Lukeš, I. *Dalton Trans.* **2008**, 3027–3047.

arm and on investigations of the properties of their Ln^{III}-complexes relevant to MRI applications. We previously communicated[18] data concerning $H_3\mathbf{L^1}$ (Chart 1) and its complexes. Here, we give full experimental details for the synthesis of $H_3\mathbf{L^1}$ as well as for a new bifunctional derivative $H_4\mathbf{L^2}$ (Chart 1) bearing an additional carboxylic group on the pyridine-*N*-oxide moiety; the properties of the complexes of both ligands are compared. The carboxylic group of $H_4\mathbf{L^2}$ allows a direct linkage to other molecules, such as dendrimers,[14] through a short and rigid amide bond. The crucial parameters determining the relaxivity were assessed on the basis of ^{1}H NMRD (nuclear magnetic relaxation dispersion), variable-temperature ^{17}O NMR relaxation measurements, ^{17}O NMR Dy-induced shifts, and luminescence measurements.

Experimental Section

Materials and Methods. *t*-Bu$_3$do3a·HBr (tris-*tert*-butyl 1,4,7,10-tetraazacyclododecane-1,4,7-trisacetate hydrobromide) was prepared according to the published procedure.[19] Gaseous H_2S was generated by the reaction of FeS with hydrochloric acid (HCl). K_2CO_3 was calcined for 2 h at 400 °C and powdered prior to use. Dry CH_3CN was obtained by distillation from P_2O_5. Tetrahydrofuran (THF) was dried by reflux with K and distilled under Ar.

Elemental analyses were performed at the Institute of Macromolecular Chemistry of the Czech Academy of Sciences (Prague, Czech Republic). The luminescence measurements were performed on an AMINCO Bowman series 2 spectrometer (lifetimes were reproducible within ±10%). NMR spectra were acquired on Varian UNITY INOVA 400 and Varian NMRS 300 spectrometers. Electrospray ionization mass spectrometry (ESI-MS) spectra were recorded on a Bruker ESQUIRE 3000 with ion-trap detection in a positive mode.

High-Performance Liquid Chromatography (HPLC). High-purity chemicals were used for HPLC experiments, namely, gradient-grade acetonitrile (Merck), deionized water, an 85% solution of H_3PO_4 (Merck), and trifluoroacetic acid (TFA; Acros). The reaction progress during the preparation of **8** was followed using a linear gradient (A:B:C, where A = CH_3CN, B = H_2O with 0.1% (by volume) of 85% H_3PO_4, C = H_2O): 10:20:70−30:20:50 in 10 min, 30:20:50 held for 5 min, and detection at 210 nm. The Ln^{III} complexes of $H_3\mathbf{L^1}$ and $H_4\mathbf{L^2}$ were analyzed on a column Luna phenyl−hexyl 150 × 4.6 mm (Phenomenex) using isocratic elution with composition 5:95 (CH_3CN/H_2O with 0.1% TFA), detection at 254 nm (complexes of $H_3\mathbf{L^1}$) and 289 nm (complexes of $H_4\mathbf{L^2}$). The flow rates were maintained at 1 mL min^{-1}.

Single-Crystal Preparation. The single crystals of $H_3\mathbf{L^1}\cdot 2HCl\cdot 4H_2O$ and $H_4\mathbf{L^2}\cdot 2HCl\cdot 2H_2O$ were prepared from aqueous solutions acidified with a few drops of concentrated aqueous HCl by a slow diffusion of acetone vapor.

X-ray Structure Determination. Selected crystals were mounted on a glass fiber in a random orientation and cooled to 150(1) K. The diffraction data were collected by employing a Nonius Kappa CCD diffractometer (Enraf-Nonius) using Mo Kα (λ = 0.710 73 Å) at 150(1) K (Cryostream Cooler Oxford Cryosystem) and analyzed using the *HKL DENZO* program package.[20] The structures were solved by direct methods and refined by full-matrix least-squares techniques (*SIR92*[21] and *SHELXL97*[22]). The scattering factors used for neutral atoms were included in the *SHELXL97* program. Selected experimental data are listed in Tables 1 and S1 in the Supporting Information.

In the structure of $H_3\mathbf{L^1}\cdot 2HCl\cdot 4H_2O$, all non-hydrogen atoms were refined anisotropically. Solvate water molecules occupy five positions, three of them with full occupancy and the last two best fitted with half-occupancy, giving in total four hydrate molecules. One chloride anion was best refined as disordered in three close positions with a relative occupancy of 70:20:10 (%, fixed). All hydrogen atoms (including those attached to water oxygen atoms) were located in the electron density difference map. To keep a low number of parameters, they were fixed in theoretical (C−H and N−H) or original (O−H) positions using $U_{eq}(H) = 1.2U_{eq}(X)$.

In the structure of $H_4\mathbf{L^2}\cdot 2HCl\cdot 2H_2O$, all non-hydrogen atoms were refined anisotropically. All hydrogen atoms (including those

(6) Aime, S.; Geninatti Crich, S.; Gianolio, E.; Giovenzana, G. B.; Tei, L.; Terreno, E. *Coord. Chem. Rev.* **2006**, *250*, 1562–1579.

(7) (a) Cheng, T.-H.; Wang, Y.-M.; Lin, K.-T.; Liu, G.-C. *J. Chem. Soc., Dalton Trans.* **2001**, 3357–3366. (b) Cheng, T.-H.; Lee, T.-M.; Ou, M.-H.; Li, C.-R.; Liu, G.-C.; Wang, Y.-M. *Helv. Chim. Acta* **2002**, *85*, 1033–1050. (c) Laus, S.; Ruloff, R.; Tóth, É.; Merbach, A. E. *Chem.−Eur. J.* **2003**, *9*, 3555–3566. (d) Burai, L.; Tóth, É.; Merbach, A. E. *Chem. Commun.* **2003**, 2680–2681. (e) Burai, L.; Tóth, É.; Sour, A.; Merbach, A. E. *Inorg. Chem.* **2005**, *44*, 3561–3568. (f) Wang, Y.-M.; Li, C.-R.; Huang, Y.-C.; Ou, M.-H.; Liu, G.-C. *Inorg. Chem.* **2005**, *44*, 382–392. (g) Ou, M.-H.; Tu, C.-H.; Tsai, S.-C.; Lee, W.-T.; Liu, G.-C.; Wang, Y.-M. *Inorg. Chem.* **2006**, *45*, 244–254. (h) Torres, S.; Martins, J. A.; André, J. P.; Geraldes, C. F. G. C.; Merbach, A. E.; Tóth, É. *Chem.−Eur. J.* **2006**, *12*, 940–948. (I) Cheng, T.-H.; Lee, W.-T.; Jeng, J.-S.; Wu, C.-M.; Liu, G.-C.; Chiang, M. Y. N.; Wang, Y.-M. *Dalton Trans.* **2006**, 5149–5155. (j) Ou, M.-H.; Chen, Y.-M.; Chang, Y.-H.; Lu, W.-K.; Liu, G.-C.; Wang, Y.-M. *Dalton Trans.* **2007**, 2749–2759. (k) Torres, S.; Martins, J. A.; André, J. P.; Pereira, G. A.; Király, R.; Brücher, E.; Helm, L.; Tóth, É.; Geraldes, C. F. G. C. *Eur. J. Inorg. Chem.* **2007**, 5489–5499. (l) Laurent, S.; Vander Elst, L.; Vroman, A.; Muller, R. N. *Helv. Chim. Acta* **2007**, *90*, 562–573.

(8) Jászberényi, Z.; Sour, A.; Tóth, É.; Benmelouka, M.; Merbach, A. E. *Dalton Trans.* **2005**, 2713–2719.

(9) Ruloff, R.; Tóth, É.; Scopelliti, R.; Tripier, R.; Handel, H.; Merbach, A. E. *Chem. Commun.* **2002**, 2630–2631.

(10) Congreve, A.; Parker, D.; Gianolio, E.; Botta, M. *Dalton Trans.* **2004**, 1441–1445.

(11) Kobayashi, H.; Brechbiel, M. W. *Curr. Pharm. Biotechnol.* **2004**, *5*, 539–549. Venditto, V. J.; Regino, C. A. S.; Brechbiel, M. W. *Mol. Pharm.* **2005**, *2*, 302–311.

(12) Langereis, S.; Dirksen, A.; Hackeng, T. M.; van Genderen, M. H. P.; Meijer, E. W. *New J. Chem.* **2007**, *31*, 1152–1160.

(13) (a) Caravan, P.; Cloutier, N. J.; Greenfield, M. T.; McDermid, S. A.; Dunham, S. U.; Bulte, J. W. M.; Amedio, J. C., Jr.; Looby, R. J.; Supkowski, R. M.; Horrocks, W. D., Jr.; McMurry, T. J.; Lauffer, R. B. *J. Am. Chem. Soc.* **2002**, *124*, 3152–3162. (b) Caravan, P.; Parigi, G.; Chasse, J. M.; Cloutier, N. J.; Ellison, J. J.; Lauffer, R. B.; Luchinat, C.; McDermid, S. A.; Spiller, M.; McMurry, T. J. *Inorg. Chem.* **2007**, *46*, 6632–6639.

(14) (a) Nicolle, G. M.; Tóth, É.; Schmitt-Willich, H.; Radüchel, B.; Merbach, A. E. *Chem.−Eur. J.* **2002**, *8*, 1040–1048. (b) Jászberényi, Z.; Moriggi, L.; Schmidt, P.; Weidensteiner, C.; Kneuer, R.; Merbach, A. E.; Helm, L.; Tóth, É. *J. Biol. Inorg. Chem.* **2007**, *12*, 406–420.

(15) (a) Laus, S.; Sour, A.; Ruloff, R.; Tóth, É.; Merbach, A. E. *Chem.−Eur. J.* **2005**, *11*, 3064–3076. (b) Lebdušková, P.; Sour, A.; Helm, L.; Tóth, É.; Kotek, J.; Lukeš, I.; Merbach, A. É. *Dalton Trans.* **2006**, 3399–3406.

(16) (a) Rudovský, J.; Hermann, P.; Botta, M.; Aime, S.; Lukeš, I. *Chem. Commun.* **2005**, 2390–2392. (b) Rudovský, J.; Botta, M.; Hermann, P.; Hardcastle, K. I.; Lukeš, I.; Aime, S. *Bioconjugate Chem.* **2006**, *17*, 975–987.

(17) Tóth, É.; Pubanz, D.; Vauthey, S.; Helm, L.; Merbach, A. E. *Chem.−Eur. J.* **1996**, *2*, 1607–1615.

(18) Polášek, M.; Rudovský, J.; Hermann, P.; Lukeš, I.; Vander Elst, L.; Muller, R. N. *Chem. Commun.* **2004**, 2602–2603.

(19) Dadabhoy, A.; Faulkner, S.; Sammes, P. G. *J. Chem. Soc., Perkin Trans. 2* **2002**, 348–357.

(20) (a) Otwinovski, Z.; Minor, W. *HKL Denzo and Scalepack Program Package*; Nonius BV: Delft, The Netherlands, 1997. (b) Otwinovski, Z.; Minor, W. *Methods Enzymol.* **1997**, *276*, 307–326.

(21) Altomare, A.; Burla, M. C.; Camalli, M.; Cascarano, G.; Giacovazzo, C.; Guagliardi, A.; Polidori, G. *J. Appl. Crystallogr.* **1994**, *27*, 435–435.

(22) Sheldrick, G. M. *SHELXL97, A Computer Program for Refinement of Crystal Structures*; University of Göttingen: Göttingen, Germany, 1997.

Table 1. Experimental Data of Reported Crystal Structures

parameter	$H_3\mathbf{L^1}\cdot 2HCl\cdot 4H_2O$	$H_4\mathbf{L^2}\cdot 2HCl\cdot 2H_2O$
formula	$C_{20}H_{41}Cl_2N_5O_{11}$	$C_{21}H_{37}Cl_2N_5O_{11}$
M	598.48	606.46
color	colorless	colorless
shape	rod	prism
crystal system	monoclinic	monoclinic
space group	$C2/c$	$P2_1/n$
a/Å	17.0443(3)	8.15240(10)
b/Å	15.2040(3)	25.3939(5)
c/Å	22.3388(3)	13.5391(3)
β/deg	101.2581(11)	104.2638(11)
U/Å^3	5677.52(17)	2716.47(9)
Z	8	4
D_c/g cm^{-3}	1.400	1.483
μ/mm^{-1}	0.291	0.306
$R1$ [$I \geq 2\sigma(I)$]; $R2$ (all data)[a]	0.0623; 0.0851	0.0361; 0.0534
$wR1$ [$I \geq 2\sigma(I)$]; $wR2$ (all data)[a]	0.1581; 0.1755	0.0862; 0.0945

[a] $R1$, $R2 = \sum|F_o - F_c|/\sum|F_c|$; $wR1$, $wR2 = [\sum w(F_o^2 - F_c^2)^2/\sum w(F_o^2)^2]^{1/2}$.[22]

attached to water oxygen atoms) were located in the electron density difference map. In the final cycles, hydrogen atoms were fixed in theoretical (C−H and N−H) or original (O−H) positions using $U_{eq}(H) = 1.2U_{eq}(X)$.

^{1}H NMRD Profiles. The ^{1}H longitudinal relaxation rates defined as $1/T_1$ were measured with a Stelar Spinmaster FFC-2000 spectrometer using the field-cycling method. The range of magnetic fields was 0.00024−0.24 T (corresponding to 0.01−10 MHz proton Larmor frequency). Additional data points at 0.47 T (20 MHz) and 1.41 T (60 MHz) were obtained with Bruker Minispec mq-20 and Bruker Minispec mq-60 relaxometers. The T_1 values were determined using the standard inversion-recovery pulse sequence. The measurements were performed at the temperatures 25 and 37 °C for both compounds; data at 5 °C were acquired only for [Gd(H$_2$O)(**L^1**)].

^{17}O NMR Variable-Temperature Measurements. The ^{17}O NMR measurements were performed on a Varian UNITY INOVA 400 spectrometer (9.4 T and 54.22 MHz). The temperature was controlled with an L-900 VT unit and calibrated on ^{1}H NMR signals of methanol and ethylene glycol.[23] The samples were enriched to ca. 0.1% of ^{17}O with the addition of $H_2{}^{17}O$ (30%, IsoTrade), and approximately 0.5% of *t*-BuOH was added. Longitudinal relaxation times were measured by a standard inversion-recovery pulse sequence. Transversal relaxation times were determined by a Carr−Purcell−Meiboom−Gill spin−echo pulse sequence. No spinning of the samples and no frequency lock were used. The bulk magnetic susceptibility (BMS) contributions to chemical shifts in the paramagnetic samples were determined from the differences of ^{1}H NMR signals of *t*-BuOH between the diamagnetic and paramagnetic sample and were subtracted. The samples were kept in the probe for at least 10 min prior to the measurement to ensure temperature equilibration.

Fitting of Data. The simultaneous analyses of ^{1}H NMRD and ^{17}O NMR variable-temperatures T_1 and T_2 and chemical shift data were performed with Micromath Scientist using the least-squares procedure (for the complete set of equations used, see the Supporting Information).

Syntheses. 2-(Chloromethyl)pyridine-1-oxide (2). The commercial 2-(chloromethyl)pyridine hydrochloride (2.0 g, 12.19 mmol) was first purified on a short column of alumina by elution with 200 mL of chloroform. Brown impurities were retained on the column. The resulting solution in a round-bottomed flask was submerged in an ice bath and stirred. A solution of *m*-chloroperoxobenzoic acid (MCPBA; 70%, 4.5 g, 18.25 mmol) was added dropwise over a period of 90 min. The mixture was then slowly warmed up to room temperature and stirred overnight. The solution was passed through an alumina column, and pure product was eluted using a mixture of 95:5 $CHCl_3$/MeOH. Faintly yellow oil was obtained after evaporation, which crystallized spontaneously. The solid was crushed, and residual solvents were removed on a rotary evaporator to give the final product (1.61 g, 92%). ^{1}H NMR (400 MHz, $CDCl_3$): δ_H 4.86 (2 H, s, −CH_2Cl), 7.28−7.32 (1 H, m, aryl), 7.33−7.37 (1 H, m, aryl), 7.63 (1 H, m, aryl), 8.29 (1 H, m, aryl). ^{13}C NMR (400 MHz, $CDCl_3$): δ_C 39.7 (1 C, −CH_2Cl), 125.2 (1 C, aryl), 125.6 (1 C, aryl), 125.8 (1 C, aryl), 139.4 (1 C, aryl), 147.2 (1 C, aryl). ESI-MS. Found (calcd): *m*/*z* 167.8 (168.0) (M + Na$^+$) ($C_6H_6{}^{37}ClNNaO$), 165.8 (166.0) (M + Na$^+$) ($C_6H_6{}^{35}ClNNaO$), 145.9 (146.0) (M + H$^+$) ($C_6H_7{}^{37}ClNO$), 143.9 (144.0) (M + H$^+$) ($C_6H_7{}^{35}ClNO$). Elem anal. Calcd for C_6H_6ClNO: C, 50.19; H, 4.21; Cl, 24.69; N, 9.76. Found: C, 50.15; H, 4.19; Cl, 24.82; N, 9.45.

Tris-*tert*-butyl 10-[(1-Oxidopyridin-2-yl)methyl]-1,4,7,10-tetraazacyclododecane-1,4,7-trisacetate (3). *t*-Bu$_3$do3a·HBr (6.0 g, 10.07 mmol), alkylating reagent **2** (1.45 g, 10.10 mmol), and K_2CO_3 (4.2 g, 30.39 mmol) were mixed together in a flask equipped with a magnetic stirring bar. The flask was flushed with Ar, and then the reaction was initiated with the addition of dry CH_3CN (300 mL). The reaction mixture was stirred vigorously at room temperature for 24 h. The solids were filtered off, and the filtrate was evaporated to dryness on a rotary evaporator. The residue was dissolved in CH_2Cl_2 (50 mL) and extracted with distilled water (3 × 100 mL). The organic solution was evaporated and the residue dried under high vacuum for several hours to yield thick, faintly orange oil (6.01 g, 96%), which was directly used in the next step. ^{1}H NMR (400 MHz, $CDCl_3$): δ_H 1.41 (18 H, s, −C(CH$_3$)$_3$), 1.45 (9 H, s, −C(CH$_3$)$_3$), 2.63 (4 H, m, ring CH$_2$), 2.77 (4 H, m, ring CH$_2$), 2.82 (4 H, m, ring CH$_2$), 2.84 (4 H, m, ring CH$_2$), 3.17 (4 H, s, CH$_2$CO), 3.31 (2 H, s, CH$_2$CO), 3.82 (2 H, s, CH$_2$py), 7.10−7.13 (1 H, m, aryl), 7.28−7.31 (1 H, m, aryl), 8.20 (1 H, m, aryl), 8.39 (1 H, m, aryl). ^{13}C NMR (400 MHz, $CDCl_3$): δ_C 27.8 (6 C, C(**C**H$_3$)$_3$), 27.9 (3 C, C(**C**H$_3$)$_3$), 52.0 (2 C, ring CH$_2$), 52.4 (2 C, ring CH$_2$), 53.0 (2 C, ring CH$_2$), 53.4 (1 C, **C**H$_2$py), 54.0 (2 C, ring CH$_2$), 56.1 (1 C, **C**H$_2$CO), 56.3 (2 C, **C**H$_2$CO), 80.2 (1 C, **C**(CH$_3$)$_3$), 80.3 (2 C, **C**(CH$_3$)$_3$), 122.9 (1 C, aryl), 126.2 (2 C, aryl, overlap), 138.5 (1 C, aryl), 151.0 (1 C, aryl), 170.5 (2 C, CH$_2$**C**O), 170.7 (1 C, CH$_2$**C**O). ESI-MS. Found (calcd): *m*/*z* 644.6 (644.4) (M + Na$^+$).

10-[(1-Oxidopyridin-2-yl)methyl]-1,4,7,10-tetraazacyclododecane-1,4,7-triacetic Acid Dihydrochloride Tetrahydrate ($H_3\mathbf{L^1}\cdot 2HCl\cdot 4H_2O$). Compound **3** (6.01 g) was dissolved in TFA (20 mL) and stirred for 24 h at room temperature. The solvent was then evaporated on a rotary evaporator. To exchange the TFA for HCl, the residue was dissolved in and evaporated with 5 M HCl (2 × 25 mL) and water (2 × 25 mL) on a rotary evaporator. The product was purified by crystallization from a concentrated aqueous solution at 4 °C and dried on air to give $H_3\mathbf{L^1}\cdot 2HCl\cdot 4H_2O$ (3.57 g, 62%). ^{1}H NMR (400 MHz, D_2O, 90 °C): δ_H 3.10−3.13 (4 H, m, ring CH$_2$), 3.19 (8 H, m, ring CH$_2$), 3.29−3.32 (4 H, m, ring CH$_2$), 3.46 (4 H, s, CH$_2$CO), 3.92 (2 H, s, CH$_2$CO), 4.47 (2 H, s, CH$_2$py), 7.54−7.58 (1 H, m, aryl), 7.63−7.67 (1 H, m, aryl), 7.69 (1 H, m, aryl), 8.26 (1 H, m, aryl). ^{13}C NMR (400 MHz, D_2O, 90 °C): δ_C 51.7 (2 C, ring CH$_2$), 52.0 (2 C, ring CH$_2$), 53.6 (2 C, ring CH$_2$), 54.1 (2 C, ring CH$_2$), 55.6 (2 C, **C**H$_2$CO), 56.2 (1 C, **C**H$_2$py), 57.2 (1 C, **C**H$_2$CO), 131.0 (1 C, aryl), 132.4 (1 C, aryl), 135.3 (1 C, aryl), 142.9 (1 C, aryl), 144.2 (1 C, aryl), 172.3 (1 C, CH$_2$**C**O), 174.5 (2 C, CH$_2$**C**O). ESI-MS. Found (calcd): *m*/*z* 454.3 (454.2) (M + H$^+$). Elem anal Calcd for $C_{20}H_{41}Cl_2N_5O_{11}$: C, 40.12; H, 6.91; Cl, 11.85; N, 11.70. Found: C, 40.32; H, 6.88; Cl, 11.85; N, 11.59.

(23) Bornais, J.; Brownstein, S. *J. Magn. Reson.* **1978**, *29*, 207–211.

Complex 5. The chelate **5** was prepared from **4** (10.96 g, 59.2 mmol) and copper(II) acetate monohydrate (5.91 g, 29.6 mmol) according to the published procedure[24] to yield 12.80 g (100%) of product. Elem anal. Calcd for $C_{14}H_{12}CuN_2O_{10}$: C, 38.94; H, 2.80; N, 6.49. Found: C, 39.10; H, 2.58; N, 6.40.

Complex 6. The complex **5** (12.80 g, 29.6 mmol) was methylated according to the published procedure[25] to give 12.32 g (90%) of **6**. Elem anal. Calcd for $C_{16}H_{16}CuN_2O_{10}$: C, 41.79; H, 3.51; N, 6.09. Found: C, 42.96; H, 2.90; N, 6.22.

Pyridine-2,4-dicarboxylic Acid 4-Methyl Ester (7). The chelate **6** (12.32 g, 26.8 mmol) was disintegrated by reaction with H_2S as described in the literature[25] and afforded pure **7** (8.40 g, 87%). ^{1}H NMR (400 MHz, CD_3OD): δ_H 3.99 (3 H, s, CH_3), 8.11 (1 H, dd, aryl, J_{HH} = 5.0 Hz, J_{HH} = 1.6 Hz), 8.58 (1 H, dd, aryl, J_{HH} = 1.6 Hz, J_{HH} = 0.8 Hz), 8.85 (1 H, dd, aryl, J_{HH} = 5.0 Hz, J_{HH} = 0.8 Hz). ^{13}C NMR (400 MHz, CD_3OD): δ_C 53.5 (1 C, CH_3), 125.1 (1 C, py), 127.4 (1 C, py), 140.7 (1 C, py), 150.4 (1 C, py), 151.5 (1 C, py), 166.0 (1 C, CO), 166.8 (1 C, CO). ESI-MS. Found (calcd): *m*/*z* 181.9 (182.0) (M + H$^+$). Elem anal. Calcd for $C_8H_7NO_4$: C, 53.04; H, 3.89; N, 7.73. Found: C, 53.23; H, 4.01; N, 7.62.

Methyl 2-(Hydroxymethyl)pyridine-4-carboxylate (8). The monoester **7** (3 g, 16.6 mmol) was dissolved in dry THF (100 mL) under Ar, and the solution was cooled to −10 °C and stirred. Then 1 M BH_3 in THF (41 mL) was added dropwise in 75 min. The reaction mixture was maintained at −10 °C for another 30 min and then allowed to warm up to room temperature. The reverse-phase HPLC showed that the product reached its maximum content approximately after 2 h of reaction at room temperature (retention times: **7**·BH_3, 7.89 min; **8**·BH_3, 11.77 min; diol·BH_3, 5.94 min). The reaction was stopped by the gradual addition of methanol (100 mL) and subsequent reflux (1 h). The solvents were removed on a rotary evaporator, and saturated aqueous $NaHCO_3$ (100 mL) was added to the oily residue. The aqueous solution was extracted with chloroform (4 × 30 mL); the organic phases were combined and dried over anhydrous Na_2SO_4. The solids were filtered off, and the solution was evaporated. The resulting oil crystallized spontaneously and gave **8** as an orange solid (1.60 g, 58%), which was used directly in the next step. For characterization purposes, a small sample was recrystallized in hot toluene and gave pure **8** as white needle-shaped crystals. ^{1}H NMR (400 MHz, $CDCl_3$): δ_H 3.80 (1 H, br s, OH), 3.97 (3 H, s, CH_3), 4.85 (2 H, s, CH_2), 7.56−7.77 (1 H, m, aryl); 7.85 (1 H, m, aryl), 8.71 (1 H, m, aryl). ^{13}C NMR (400 MHz, $CDCl_3$): δ_C 52.8 (1 C, CH_3), 64.2 (1 C, CH_2), 119.8 (1 C, aryl), 121.6 (1 C, aryl), 138.0 (1 C, aryl), 149.3 (1 C, aryl), 160.4 (1 C, aryl), 165.5 (1 C, CO). ESI-MS. Found (calcd): *m*/*z* 167.9 (168.1) (M + H$^+$). Elem anal. Calcd for $C_8H_9NO_3$: C, 57.48; H, 5.43; N, 8.38. Found: C, 57.39; H, 5.48; N, 8.23.

Methyl 2-(Chloromethyl)pyridine-4-carboxylate Hydrochloride (9). The procedure reported by Scopes and co-workers[26] was utilized with modifications. The alcohol **8** (1.14 g, 6.82 mmol) was added gradually in small portions to stirred thionyl chloride (12 mL) at 0 °C. After dissolution, the flask was closed with a calcium chloride tube and the reaction mixture stirred for 24 h at room temperature. Thionyl chloride was then removed on a rotary evaporator. The residue was dissolved in chloroform (10 mL), and the solution was evaporated again (repeated two times). The resulting oil solidified within 1 h. The solid was crushed, and residual solvents were removed on a rotary evaporator. The resulting brownish powder (1.51 g, 100%) was directly used in the next step. ^{1}H NMR (400 MHz, $CDCl_3$): δ_H 4.09 (3 H, s, CH_3), 5.25 (2 H, s, CH_2), 8.38 (1 H, dd, aryl, J_{HH} = 5.8 Hz, J_{HH} = 1.7 Hz), 8.55 (1 H, d, aryl, J_{HH} = 1.7 Hz), 9.00 (1 H, d, aryl, J_{HH} = 5.8 Hz). ^{13}C NMR (400 MHz, $CDCl_3$): δ_C 40.0 (1 C), 50.0 (1 C), 125.4 (1 C, aryl), 126.3 (1 C, aryl), 143.0 (1 C, aryl), 144.9 (1 C, aryl), 153.8 (1 C, aryl), 162.2 (1 C, CO). ESI-MS. Found (calcd): *m*/*z* 187.9 (188.0) (M + H$^+$) ($C_8H_9{}^{37}ClNO_2$), 185.9 (186.0) (M + H$^+$) ($C_8H_9{}^{35}ClNO_2$).

Methyl 2-(Chloromethyl)-1-oxidopyridine-4-carboxylate (10). The procedure was analogous to the preparation of **2**. Starting with **9** (1.51 g, 6.80 mmol), it afforded crude **10** as a brownish solid. Pure **10** was obtained by recrystallization from hot toluene as a white crystalline powder (1.09 g, 79%). ^{1}H NMR (400 MHz, $CDCl_3$): δ_H 3.90 (3 H, s, CH_3), 4.74 (2 H, s, CH_2), 7.81 (1 H, dd, aryl, J_{HH} = 6.7 Hz, J_{HH} = 2.1 Hz), 8.14 (1 H, d, aryl, J_{HH} = 2.1 Hz), 8.22 (1 H, d, aryl, J_{HH} = 6.7 Hz). ^{13}C NMR (400 MHz, $CDCl_3$): δ_C 39.4 (1 C), 52.9 (1 C), 125.3 (1 C, aryl), 126.0 (1 C, aryl), 126.4 (1 C, aryl), 139.6 (1 C, aryl), 147.6 (1 C, aryl), 163.7 (1 C, CO). ESI-MS. Found (calcd): *m*/*z* 225.9 (226.0) (M + Na$^+$) ($C_8H_8{}^{37}ClNNaO_3$), 223.9 (224.0) (M + Na$^+$) ($C_8H_8{}^{35}ClNNaO_3$), 203.9 (204.0) (M + H$^+$) ($C_8H_9{}^{37}ClNO_3$), 201.9 (202.0) (M + H$^+$) ($C_8H_9{}^{35}ClNO_3$). Elem anal. Calcd for $C_8H_9NO_3$: C, 47.66; H, 4.00; Cl, 17.59; N, 6.95. Found: C, 47.61; H, 3.86; Cl, 17.54; N, 6.76.

Tris-*tert*-butyl 10-{[4-(Methoxycarbonyl)-1-oxidopyridin-2-yl]methyl}-1,4,7,10-tetraazacyclododecane-1,4,7-trisacetate (11). *t*-Bu_3do3a·HBr (2.95 g, 4.96 mmol), **10** (1.00 g, 4.96 mmol), and K_2CO_3 (2.06 g, 14.91 mmol) were mixed in an Ar atmosphere, and 120 mL of dry acetonitrile was added. The mixture was stirred for 24 h at room temperature. The workup was analogous to that of **3**. The reaction afforded **11** as a pale-orange viscous oil (3.30 g, 98%), which was used directly in the next step. ^{1}H NMR (400 MHz, $CDCl_3$): δ_H 1.40 (18 H, s, −C(CH_3)$_3$), 1.44 (9 H, s, −C(CH_3)$_3$), 2.68 (4 H, m, ring CH_2), 2.84 (4 H, m, ring CH_2), 2.88 (8 H, m, ring CH_2), 3.20 (4 H, s, CH_2CO), 3.31 (2 H, s, CH_2CO), 3.81 (2 H, s, CH_2py), 3.93 (3 H, s, CH_3), 7.73−7.75 (1 H, m, aryl), 8.20−8.22 (1 H, m, aryl), 8.73 (1 H, m, aryl). ^{13}C NMR (400 MHz, $CDCl_3$): δ_C 28.09 (6 C, C(**C**H$_3$)$_3$), 28.13 (3 C, C(**C**H$_3$)$_3$), 52.1 (2 C, ring CH_2), 52.47 (1 C, CH_3), 52.54 (2 C, ring CH_2), 52.8 (2 C, ring CH_2), 54.0 (2 C, CH_2py), 54.1 (2 C, ring CH_2), 56.2 (2 C, **C**H$_2$CO), 56.6 (1 C, **C**H$_2$CO−), 80.6 (1 C, **C**(CH$_3$)$_3$), 80.7 (2 C, **C**(CH$_3$)$_3$), 123.5 (1 C, CH aryl), 126.1 (1 C, CH aryl), 126.5 (1 C, aryl), 139.2 (1 C, CH aryl), 152.0 (1 C, aryl), 164.5 (1 C, py**C**O), 170.9 (2 C, CH$_2$**C**O); 171.0 (1 C, CH$_2$**C**O). ESI-MS. Found (calcd): *m*/*z* 680.6 (680.4) (M + H$^+$).

10-[(4-Carboxy-1-oxidopyridin-2-yl)methyl]-1,4,7,10-tetraazacyclododecane-1,4,7-triacetic Acid Dihydrochloride Dihydrate (H_4L^2·2HCl·2H$_2$O). The ester **11** (3.3 g) was dissolved in 20 mL of a methanol/water (1:1) mixture, and lithium hydroxide monohydrate (0.250 g, 5.96 mmol) was added. The mixture was stirred until complete dissolution of the hydroxide. The solvents were removed on a rotary evaporator, and the residue was dissolved in 10 mL of TFA and stirred for 24 h at room temperature. The workup was analogous to that of H_3L^1. The product was obtained as a white crystalline powder (1.98 g, 67%). ^{1}H NMR (300 MHz, D_2O, 90 °C): δ_H 3.21−3.28 (4 H, m, ring CH_2), 3.30−3.35 (8 H, m, ring CH_2), 3.35−3.41 (4 H, m, ring CH_2), 3.63 (4 H, s, CH_2CO), 3.92 (2 H, s, CH_2CO), 4.56 (2 H, s, CH_2py), 8.07−8.10 (1 H, m, aryl), 8.24 (1 H, m, aryl), 8.42−8.44 (1 H, m, aryl). ^{13}C NMR (300 MHz, D_2O, 90 °C): δ_C 51.9 (2 C, ring CH_2), 52.3 (2 C, ring CH_2), 53.7 (2 C, ring CH_2), 53.9 (2 C, ring CH_2), 56.0 (2 C, **C**H$_2$CO), 56.2 (1 C, **C**H$_2$py), 57.6 (1 C, **C**H$_2$CO), 130.9 (1 C, aryl), 132.4 (1 C, aryl),

(24) Lukeš, R.; Jureček, M. *Collect. Czech. Chem. Commun.* **1948**, *13*, 131–160.
(25) Ooi, G. K. S.; Magee, R. J. *J. Inorg. Nucl. Chem.* **1970**, *32*, 3315–3320.
(26) Scopes, D. I. C.; Hayes, N. F.; Bays, D. E.; Belton, D.; Brain, J.; Brown, D. S.; Judd, D. B.; Mcelroy, A. B.; Meerholz, C. A.; Naylor, A.; Hayes, A. G.; Sheehan, M. J.; Birch, P. J.; Tyers, M. B. *J. Med. Chem.* **1992**, *35*, 490–501.

Scheme 1. Synthesis of $H_3\mathbf{L}^1$ and $H_4\mathbf{L}^2$

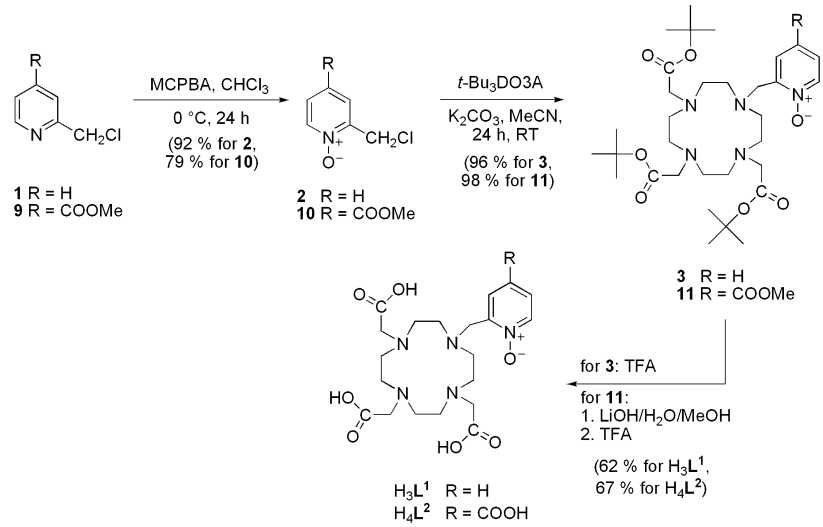

133.8 (1 C, aryl), 143.5 (1 C, aryl), 144.7 (1 C, aryl), 168.7 (1 C, py**C**O), 172.6 (1 C, CH_2**C**O), 174.6 (2 C, CH_2**C**O). ESI-MS. Found (calcd): *m*/*z* 498.1 (498.2) ($M + H^+$). Calcd for $C_{21}H_{37}Cl_2N_5O_{11}$: C, 41.59; H, 6.15; Cl, 11.69; N, 11.55. Found: C, 41.10; H, 6.12; Cl, 11.96; N, 11.88.

Preparation of the Ln^{III} Complexes. The complexes of $H_3\mathbf{L}^1$ and $H_4\mathbf{L}^2$ were prepared by dissolving lanthanide(III) chloride and 1.05−1.10 equiv of the ligand in a small amount of distilled water. The pH was adjusted to 7 with 2 M KOH, and the mixture was stirred for 24 h at room temperature. All samples were checked using the xylenol orange test (urotropine buffer, pH 5.0) to exclude the presence of free Ln^{III} ions. The solutions of the complexes were used without further purification. The exact concentrations of the complexes in the final samples were determined by measuring the bulk magnetic susceptibility shift of the ^{1}H NMR signal of *t*-BuOH.[27] For this purpose, ca. 0.5% of *t*-BuOH was added to the samples. Molecular peaks observed in MS were in accordance with the predicted masses and reflected the theoretical isotopic distribution of the lanthanides (Table S7 in the Supporting Information). All samples were analyzed by reversed-phase HPLC and by mass spectrometry. In all cases, only one metal-containing compound was observed by HPLC, which could be clearly distinguished from the excessive ligand (Table S8 and Figure S6 in the Supporting Information).

Results and Discussion

Syntheses. Both ligands were obtained by alkylation of *t*-Bu_3do3a[19] with a corresponding alkylating agent (**2** or **10**) and subsequent deprotection of the carboxylic groups (Scheme 1). The alkylating agents **2** and **10** were prepared by oxidation of (chloromethyl)pyridines **1** and **9** with *m*-chloroperoxobenzoic acid and were obtained in a pure state by crystallization. Unlike the previously reported conditions,[18] it was found that elevated temperature is not essential to the completion of alkylation of *t*-Bu_3do3a. In fact, 1 equiv of the alkylating reagent and 24 h of reaction time at room temperature gave high-purity products in virtually quantitative yields. Hydrolysis of *tert*-butyl esters in **3** and **11** was achieved by treatment with TFA. In the case of **11**, base-catalyzed hydrolysis of pyridinecarboxylic methyl ester preceeded cleavage of *tert*-butyl esters because these two types of esters hydrolyze under different conditions. After displacement of TFA with HCl, both final products crystallized from concentrated aqueous solutions as dihydrochloride hydrates (according to elemental analyses).

The preparation of the precursor **9** started from commercial pyridine-2,4-dicarboxylic acid **4** and required several steps (Scheme 2). First, the 4-carboxylic group was methylated by utilizing selective protection of the 2-carboxylate in the copper(II) chelate **5**.[24,25] After liberation of the monomethyl ester **7** from the chelate **6** by reaction with hydrogen sulfide,[25] the free 2-carboxylic group was reduced to alcohol **8** using BH_3·THF as the adduct. This reduction seemed to be a critical step of the synthesis, and variable yields were obtained depending on the conditions. Part of the BH_3 reagent is consumed by the formation of a stable adduct with the pyridine nitrogen atom of the reactant. This probably leads to deactivation of the neighboring carboxylic group toward reduction. Simultaneous reduction of the methyl ester also takes place and contributes to a significant loss of the product as a result of the formation of a diol. The best results were obtained when the progress of the reaction was monitored by HPLC, and the reaction was stopped when the product reached its maximum content, giving isolated yields of approximately 60%. The subsequent chlorination of the alcohol **8** with thionyl chloride gave (chloromethyl)pyridine **9**.[26]

Solutions of the Ln^{III} complexes were prepared with a slight molar excess of the ligand (ca. 5−10%) to avoid any presence of free Ln^{III} ions. The appropriate amounts of lanthanide(III) chloride and the ligand were mixed together in a small amount of distilled water, the pH was adjusted to 7 with a hydroxide solution, and the reaction mixture was stirred overnight at room temperature. After this time, the samples gave a negative reaction with a xylenol orange indicator, showing that complexation was completed. The HPLC analyses proved that only one complex was formed in all cases and the MS spectra were in accordance with

(27) Corsi, D. M.; Platas-Iglesias, C.; van Bekkum, H.; Peters, J. A. *Magn. Reson. Chem.* **2001**, *39*, 723–726.

Scheme 2. Synthesis of the H_4L^2 Precursor **9**

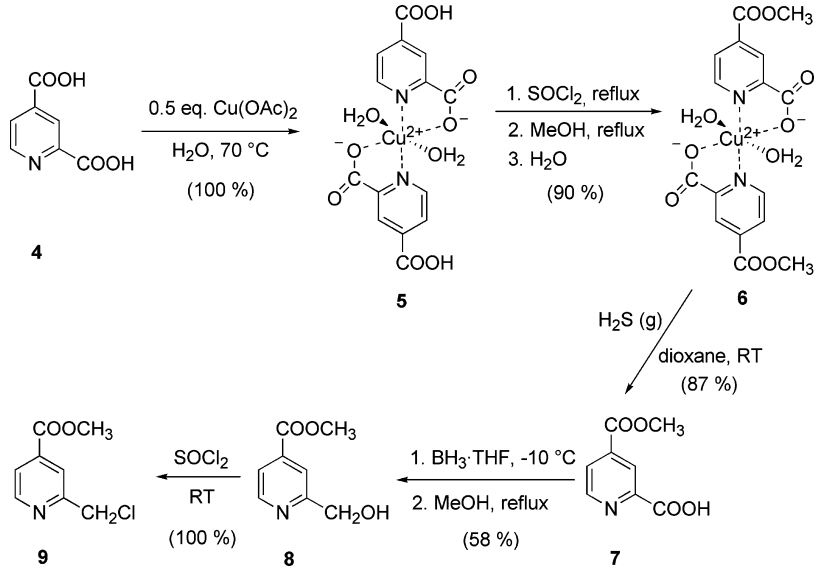

expected molecular weights. The prepared solutions were directly used for the measurements.

Crystal Structures. The single crystals were successfully prepared and analyzed by X-ray diffraction in the cases of hydrochlorides of both title ligands, $H_3\mathbf{L^1}\cdot 2HCl\cdot 4H_2O$ (CCDC-710313) and $H_4\mathbf{L^2}\cdot 2HCl\cdot 2H_2O$ (CCDC-710312). In addition, the structures of **8**·HCl (CCDC-710310) and of the Na^+ complex $H_3\mathbf{L^1}\cdot HBr\cdot 0.5NaBr\cdot 11.25H_2O$ (CCDC-710311) were determined (see the Supporting Information).

Compound $H_3\mathbf{L^1}$ crystallized in the form of dihydrochloride tetrahydrate. All three carboxylic pendant arms, as well as two nitrogen atoms of the macrocycle (those mutually *trans*, bearing acetic pendant arms), are protonated. The conformation of the macrocycle is (3,3,3,3)-B, and all substituents are oriented in the same direction from the plane of the macrocycle as it is the most common for tetrasubstituted derivatives (Figure 1).[28] The molecular conformation is stabilized by intramolecular hydrogen bonds between protonated (N4 and N10) and unprotonated (N1 and N7) nitrogen atoms N···N′ (distances 2.90−2.98 Å and angles N−H···N′ about 111°), similar to that found in other structures of substituted cyclenes with diprotonated rings [e.g., $(H_6dota)Cl_2\cdot 5H_2O$,[29] $H_5do3ap\cdot 4H_2O$,[30] tetrakis(carboxyethyl)-dota derivative,[31] or $(Et_4H_2dota)(BF_4)_2$[32]]. The acetate group attached to the unprotonated nitrogen atom N7 is turned in toward the macrocycle and participates in the hydrogen-bond system [d(O412···N10) = 3.06 Å; ∠(O412···H111−N10) = 129°]. The pyridine-*N*-oxide group is turned outward from the macrocycle cavity, with a N22−O22N bond of 1.34 Å. The whole structure is stabilized by an extensive intermolecular hydrogen-bond network between ligand molecules, chloride anions, and solvate water molecules. Selected hydrogen-bond geometries are listed in Table S3 in the Supporting Information.

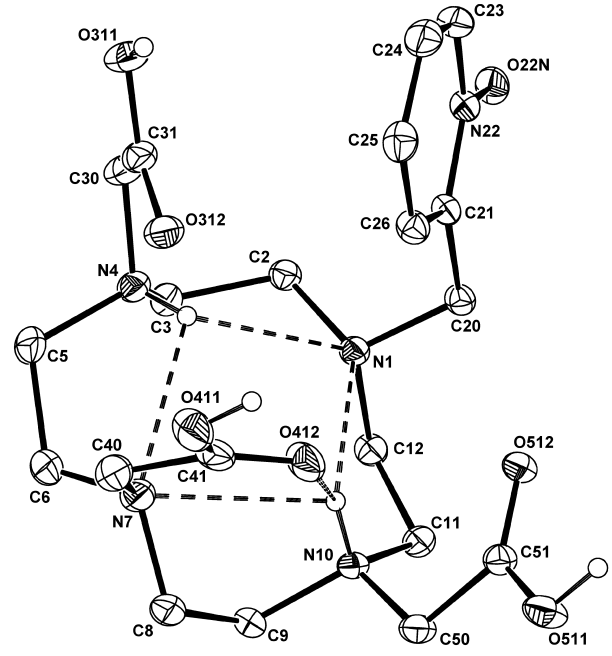

Figure 1. Molecular structure of the $(H_5\mathbf{L^1})^{2+}$ cation found in the structure of $H_3\mathbf{L^1}\cdot 2HCl\cdot 4H_2O$ showing an intramolecular hydrogen-bond system. Hydrogen atoms attached to carbon atoms are omitted for the sake of clarity.

Compound $H_4\mathbf{L^2}$ was isolated in the form of dihydrochloride dihydrate. Similarly to the previous case, all (in this case four) carboxylic groups are protonated, together with two nitrogen atoms of the macrocycle. Contrary to the previous ligand, nitrogen atoms bearing the pyridine moiety (N1) and the transannular one (N7) are protonated in this case. The conformation of the macrocycle is (3,3,3,3)-B, and all substituents are oriented in the same direction relative to

(28) Meyer, M.; Dahaoui-Gindrey, V.; Lecomte, C.; Guilard, R. *Coord. Chem. Rev.* **1998**, *178−180*, 1313–1405.
(29) Aime, S.; Barge, A.; Bruce, J. I.; Botta, M.; Howard, J. A. K.; Moloney, J. M.; Parker, D.; de Sousa, A. S.; Woods, M. *J. Am. Chem. Soc.* **1999**, *121*, 5762–5771.
(30) Táborský, P.; Lubal, P.; Havel, J.; Kotek, J.; Hermann, P.; Lukeš, I. *Collect. Czech. Chem. Commun.* **2005**, *70*, 1909–1942.
(31) Woods, M.; Aime, S.; Botta, M.; Howard, J. A. K.; Moloney, J. M.; Navet, M.; Parker, D.; Port, M.; Rousseaux, O. *J. Am. Chem. Soc.* **2000**, *122*, 9781–9792.
(32) Kobayashi, K.; Tsuboyama, S.; Tsuboyama, K.; Sakurai, T. *Acta Crystallogr., Sect.C: Cryst. Struct. Commun.* **1994**, *50*, 306–312.

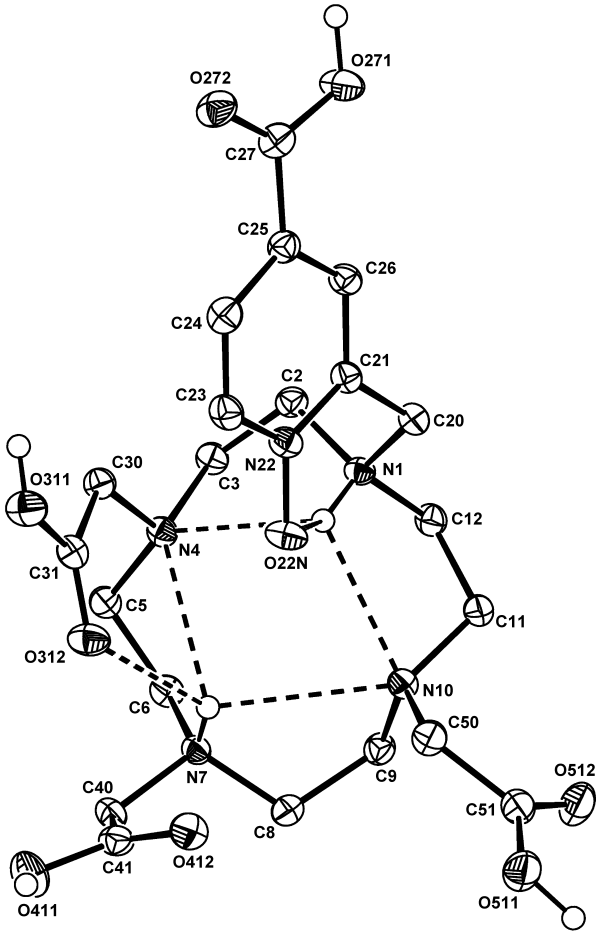

Figure 2. Molecular structure of the $(H_6\mathbf{L}^2)^{2+}$ cation found in the structure of $H_4\mathbf{L}^2 \cdot 2HCl \cdot 2H_2O$ showing an intramolecular hydrogen-bond system. Hydrogen atoms attached to carbon atoms are omitted for the sake of clarity.

the macrocycle, similarly to the previous case (Figure 2).[28] The molecule conformation is stabilized by intramolecular hydrogen bonds between protonated (N1 and N7) and unprotonated (N4 and N10) nitrogen atoms N···N′ (distances 2.87−2.94 Å and angles N−H···N′ about 110°). The acetate group attached to unprotonated nitrogen atom N4 is turned in toward the macrocycle and participates in the hydrogen-bond system [d(O312···N7) = 2.98 Å; ∠(O412···H111−N10) = 126°]. The pyridine-*N*-oxide group is also turned in toward the macrocycle cavity and forms a six-membered cycle via a hydrogen bond to nitrogen atom N1 [d(O22N···N1) = 2.77 Å; ∠(O22N···H11−N1) = 125°]. The introduction of a carboxylate function to the pyridine ring led to a slight shortening of the N−O bond to 1.31 Å in comparison with the previous structure. Similarly to the previous case, an extensive intermolecular hydrogen-bond network between ligand molecules, chloride anions, and solvate water molecules stabilizes the whole structure. Selected hydrogen-bond geometries are listed in Table S4 in the Supporting Information.

The difference found in the protonation places of both ligands is rather unexpected because the change in the ligand chemical structures takes place far away from the amino group in question. In general, when an unsymmetrically substituted cyclene skeleton is double-protonated, the first proton is located on the most basic amino group (e.g., a secondary one in the case of $(H_5do3a)SO_4 \cdot 2H_2O$[33] or that bearing an electron-donating phosphonate moiety in $H_5do3ap \cdot 4H_2O$[30]). Because of an electrostatic repulsion, the second proton occupies the *trans* nitrogen with respect to the first one. The molecules of $H_3\mathbf{L}^1$ and $H_4\mathbf{L}^2$ differ in substitution in the 4 position of the pyridine ring. Although this modification might have an effect on the resulting basicity of the nitrogen atom bearing the pyridine-*N*-oxide moiety, the difference should be small. The resulting protonation schemes are thus directed mainly by the hydrogen-bond networks allowed in the systems. In this respect, the main difference between the structures is participation of the pyridine-*N*-oxide in an intramolecular hydrogen bond to the protonated N1 atom, which occurs in the cation $(H_6\mathbf{L}^2)^{2+}$. In the cation $(H_5\mathbf{L}^1)^{2+}$, the *N*-oxide group is turned away from the macrocycle because of a very strong intermolecular hydrogen bond to a neighboring molecule (Table S3 in the Supporting Information). A hydrogen bond to N1 thus cannot be formed, and the protonation scheme changes (protonated atoms N4 and N10). However, the intramolecular hydrogen bond to the N1 atom exists in the crystal structure of $H_3\mathbf{L}^1 \cdot HBr \cdot 0.5NaBr \cdot 11.25H_2O$ (Figure S3 in the Supporting Information), and as a consequence, the protonation scheme in this structure switches to that of the cation $(H_6\mathbf{L}^2)^{2+}$ (protonated atoms N1 and N7). The position of the pyridine-*N*-oxide pendant arm is thus determined mainly by the crystal packing, which, as a consequence, affects the protonation scheme.

Excitation and Emission Spectra of the Eu^{III} Complexes. In order to determine the appropriate wavelengths of excitation and emission radiation for luminescence lifetime measurements (see below), we have first examined the excitation and emission spectra of the Eu^{III} complexes of $H_3\mathbf{L}^1$ and $H_4\mathbf{L}^2$. The spectra of the two complexes were nearly identical and, therefore, only the complex $[Eu(H_2O)(\mathbf{L}^1)]$ will be discussed (for spectra of $[Eu(H_2O)(\mathbf{L}^2)]^-$, see Figure S4 in the Supporting Information). The maximum in the excitation spectrum was found at 396 nm, and the emission spectrum showed a maximum at 616 nm (Figure 3). Those wavelengths were used in luminescence lifetime measurements. The emission peak at 616 nm belongs to the "hypersensitive" $^7F_2 \leftarrow {}^5D_0$ transition, which generally becomes dominant for complexes of low symmetry.[2,34] In our case, the C_4 symmetry of the parent DOTA complex was perturbed by the introduction of the pyridine-*N*-oxide pendant arm, resulting in a less symmetrical structure.

Determination of the Number of Inner-Sphere Water Molecules. One of the key parameters, the number of inner-sphere water molecules (q), was determined in solution by two independent techniques. The methods rely on the close chemical resemblance of the Ln^{III} ions and utilize the Eu^{III} and Dy^{III} complexes. In the first technique, q was determined

(33) Kumar, K.; Chang, C. A.; Francesconi, L. C.; Dischino, D. D.; Malley, M. F.; Gougoutas, J. Z.; Tweedle, M. F. *Inorg. Chem.* **1994**, *33*, 3567–3575.
(34) Bryden, C. C.; Reilley, C. N. *Anal. Chem.* **1982**, *54*, 610–615.

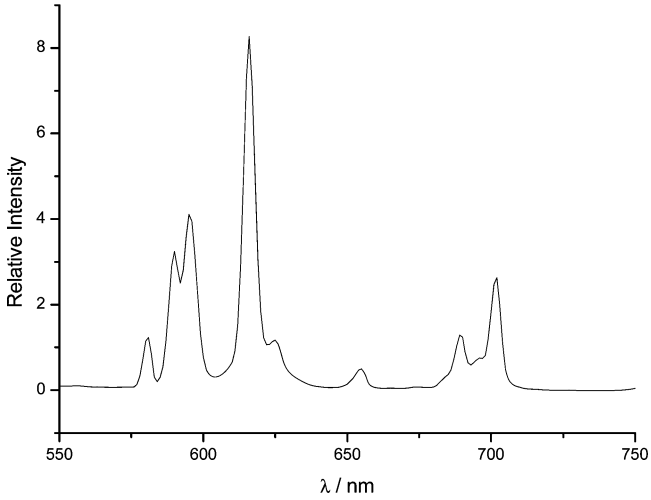

Figure 3. Emission spectrum of the $[Eu(H_2O)(\mathbf{L^1})]$ complex. The excitation wavelength was 396 nm.

from the difference between luminescence lifetimes of the excited state of the Eu^{III} ion measured in H_2O and D_2O.[35−37] The luminescence decays were monoexponential and fits resulted in the lifetime values $\tau_H = 0.624$ ms (in H_2O) and $\tau_D = 1.901$ ms (in D_2O) for the Eu^{III} complex of $H_3\mathbf{L^1}$ and $\tau_H = 0.617$ ms and $\tau_D = 1.525$ ms for the Eu^{III} complex of $H_4\mathbf{L^2}$. Several equations have been derived to calculate the number of coordinated water molecules from the luminescence lifetimes. The equation proposed by Horrocks and Sudnick[38] was revised to allow for the outer-sphere contribution (i.e., "closely diffusing water molecules") and other types of nearby oscillators.[36,37] Surprisingly, in our case, the revised equations[36,37] led to somewhat underestimated values (∼0.7−0.9), while the unrevised equation gave near-integer q values (1.13 for $[Eu(H_2O)(\mathbf{L^1})]$ and 1.03 for $[Eu(H_2O)(\mathbf{L^2})]^-$). There are two possible explanations for such an observation. First, the contribution of the outer sphere is probably smaller for electroneutral chelates (not considering the distant extra carboxylate in $[Eu(H_2O)(\mathbf{L^2})]^-$), especially if the presence of a relatively hydrophobic pyridine unit in the vicinity of the Eu^{III} ion is taken into account. Second, the efficiency of the quenching process decreases with increasing Eu−H distance.[36] The results are thus consistent with the fast water exchange rates found in the Gd^{III} complexes (vide infra), which mean destabilized and, hence, longer Gd···OH_2 bonds. The third possibility is a hydration equilibrium between $q = 0$ and 1 species in solution. However, this possibility was excluded by UV−vis measurements of the Eu^{III} complexes.[39] In any case, the values are within the error of the technique and point to one coordinated water molecule in both complexes.

To further confirm the outcome of the luminescence measurements, we used another technique to determine q independently. This method employs the ability of the Dy^{III} ions to induce an additional chemical shift of the ^{17}O NMR signal of water. The magnitude of this Dy^{III}-induced shift is linearly dependent on the concentration of the complex, with the value of the slope being related to q.[40] The $[Dy(H_2O)_8]^{3+}$ ions are usually used as a standard.[41] Under our experimental conditions, the aqueous solution of $DyCl_3$ gave the slope of −390 ppm mM^{-1}, which corresponds to the average contribution of −49 ppm mM^{-1} per one water molecule. The values determined for Dy^{III} complexes of $H_3\mathbf{L^1}$ and $H_4\mathbf{L^2}$ were −49 and −52 ppm mM^{-1}, respectively, resulting in $q = 1.0$ for $[Dy(H_2O)(\mathbf{L^1})]$ and 1.1 for $[Dy(H_2O)(\mathbf{L^2})]^-$. One inner-sphere water molecule was thus confirmed in solutions of both Dy^{III} complexes.

Having proven a direct coordination of one water molecule in the Ln^{III} complexes on both sides of Gd^{III} in the Ln series, it is generally accepted that it is the same for the Gd^{III} complexes of $H_3\mathbf{L^1}$ and $H_4\mathbf{L^2}$.

^{1}H and ^{17}O Relaxometric Measurements. The mean residential time of water molecules (τ_M) and the rotational correlation time (τ_R) as well as other parameters governing the relaxivity were determined from ^{1}H NMRD (nuclear magnetic resonance dispersion) profiles and variable-temperature ^{17}O NMR studies of water in the presence of the Gd^{III} complexes. In ^{1}H NMRD, one observes the longitudinal relaxivity of water protons as a function of the magnetic field. In the ^{17}O experiments, both longitudinal and transversal ^{17}O NMR relaxation rates and chemical shifts are measured as a function of the temperature. A multiparametrical fit of the data according to the equations of the Solomon-Bloembergen-Morgan (SBM) theory of paramagnetic relaxation provides a good estimation of the values of the investigated parameters.

In order to reduce the number of variables in the fit, some of the parameters were set to fixed values either determined by independent techniques or adopted from the data published for the Gd^{III} complex of DOTA. Thus, the values of E_v and E_R were fixed to 1 and 16.1 kJ,[42] respectively. The hyperfine coupling constant ($A/\hbar = -3.75 \times 10^6$ rad s^{-1}) was calculated from the contact contribution of the Ln-induced shift of the ^{17}O NMR signal of water in the presence of $[Ln(H_2O)(\mathbf{L^1})]$ complexes.[18] The Gd−H and Gd−O distances were fixed to values reported for similar compounds ($r_{GdH} = 3.1$ Å; $r_{GdO} = 2.5$ Å).[43] The distance for the closest approach of the outer-sphere water molecules was fixed to $A = 3.5$ Å. The quadrupolar coupling constant term was adjusted to the value reported for pure water [$\chi(1 + \eta^{2/3})^{1/2} = 7.58$ MHz][42] in the case of $[Gd(H_2O)(\mathbf{L^1})]$; however, for $[Gd(H_2O)(\mathbf{L^2})]^-$, it led to a poor agreement of the fit with

(35) Horrocks, W. D., Jr.; Sudnick, D. R. *J. Am. Chem. Soc.* **1979**, *101*, 334–340.
(36) Beeby, A.; Clarkson, I. M.; Dickins, R. S.; Faulkner, S.; Parker, D.; Royle, L.; de Sousa, A. S.; Williams, J. A. G.; Woods, M. *J. Chem. Soc., Perkin Trans. 2* **1999**, 493–503.
(37) Supkowski, R. M.; Horrocks, W. D., Jr. *Inorg. Chim. Acta* **2002**, *340*, 44–48.
(38) Horrocks, W. D., Jr.; Sudnick, D. R. *Acc. Chem. Res.* **1981**, *14*, 384–392.
(39) Polášek, M.; Kotek, J.; Hermann, P.; Císařová, I.; Binnemans, K.; Lukeš, I. *Inorg. Chem.* **2008**, *48*, 466−475.
(40) Alpoim, M. C.; Urbano, A. M.; Geraldes, C. F. G. C.; Peters, J. A. *J. Chem. Soc., Dalton Trans.* **1992**, 463–467.
(41) Djanashvili, K.; Peters, J. A. *Contrast Med. Mol. Imaging* **2007**, *2*, 67–71.
(42) Powell, D. H.; Dhubhghaill, O. M. N.; Pubanz, D.; Helm, L.; Lebedev, Y. S.; Schlaepfer, W.; Merbach, A. E. *J. Am. Chem. Soc.* **1996**, *118*, 9333–9346.
(43) Caravan, P.; Astashkin, A. V.; Raitsimring, A. M. *Inorg. Chem.* **2003**, *42*, 3972–3974.

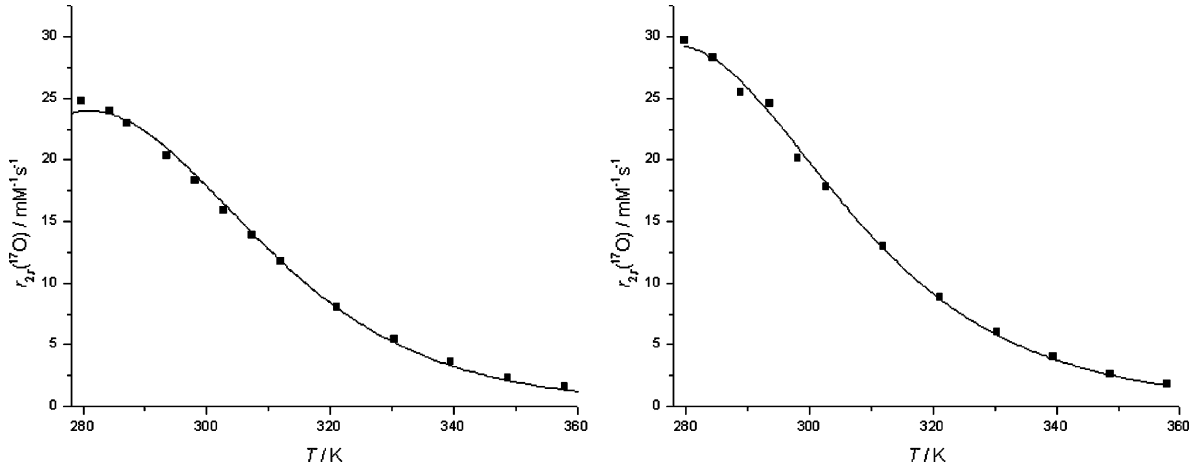

Figure 4. Variable-temperature ^{17}O NMR transversal relaxation rates per 1 mM of Gd^{III} in solutions of [$Gd(H_2O)(\mathbf{L^1})$] (left) and [$Gd(H_2O)(\mathbf{L^2})$]$^-$ (right). The concentrations of the samples were 98.5 and 70.8 mM, respectively. The curves represent results of simultaneous fits of the experimental data.

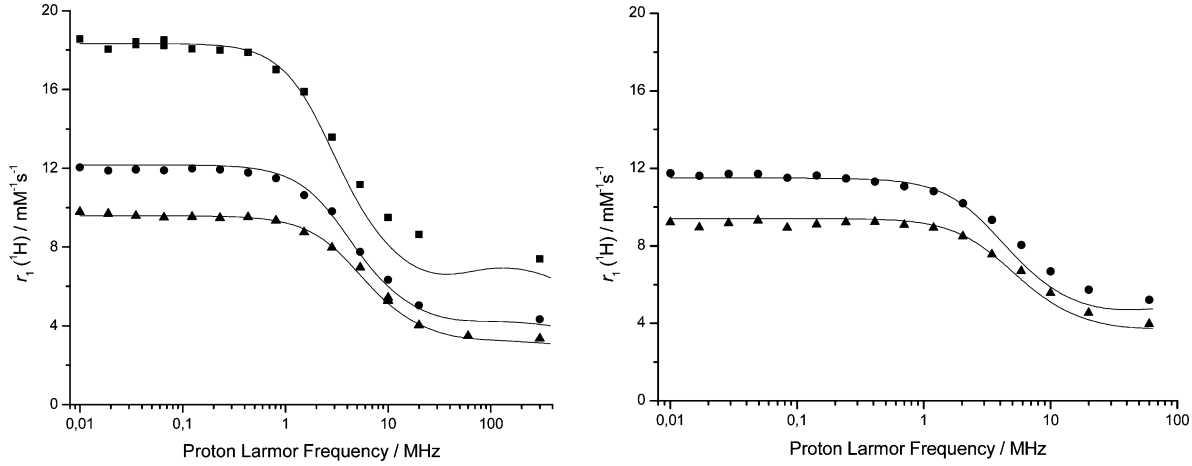

Figure 5. ^{1}H NMRD profiles of [$Gd(H_2O)(\mathbf{L^1})$] (left) and [$Gd(H_2O)(\mathbf{L^2})$]$^-$ (right) at 5 °C (squares), 25 °C (circles), and 37 °C (triangles). The concentrations of the samples were 3.32 and 1.02 mM, respectively. The curves represent results of simultaneous fits of the experimental data.

Table 2. Relaxometric Parameters for [$Gd(H_2O)(\mathbf{L^1})$] and [$Gd(H_2O)(\mathbf{L^2})$]$^-$ and Similar Complexes

parameter	[$Gd(H_2O)(\mathbf{L^1})$] [a]	[$Gd(H_2O)(\mathbf{L^2})$]$^-$[a]	[$Gd(H_2O)$(dota)]$^-$	[$Gd(H_2O)$(do3a-ce)]$^-$[b]	[$Gd(H_2O)$(do3a-hp)][c]
$^{310}r_1$/mmol^{-1} s^{-1}[d]	4.04	4.54	3.5[c]		3.6
$^{298}\tau_M$/ns	39 ± 1	34 ± 1	244[e]	16	217[f]
ΔH_M/kJ mol^{-1}	51 ± 2	46 ± 2	50[e]	39.2	49.3
$^{298}\tau_R$/ps	74 ± 3	93 ± 13	77[e]	153	51[f]
E_R/kJ mol^{-1}	16.1	16.1	16.1[e]	22.4	
$^{298}\tau_v$/ps	2.7 ± 0.1	4.7 ± 0.6	11[e]	7.0	7.5[f]
$\Delta^2/10^{20}$ s^{-2}	0.69 ± 0.03	0.90 ± 0.11	0.16[e]	0.97	0.64
$(A/\hbar)/10^6$ rad s^{-1}	−3.75	−3.75	−3.7[e]	−3.3	−2.9
q	1	1	1	1	1

[a] Underlined numbers were fixed during the fitting. [b] Reference 8. [c] Reference 44. [d] Millimolar relaxivity at 37 °C and 20 MHz. [e] Reference 42. [f] Values for 310 K.

^{17}O T_1 data and, therefore, was allowed to vary [$\chi(1 + \eta^{2/3})^{1/2} = 13.8 \pm 4.4$ MHz]. The contribution of second-sphere water molecules to ^{1}H NMR relaxivity was proven to be negligible, and only the inner- and outer-sphere terms were included in the model.

The qualitative examination of the experimental temperature dependences of the ^{17}O NMR transversal relaxivities reveals that both systems studied are in the fast water exchange regime because the maxima of the curves are located in the low-temperature region (Figure 4).[42] (For variable-temperature ^{17}O T_1 and chemical shift data, see the Supporting Information.) The shape of the ^{1}H NMRD curves (Figure 5) is typical of low-molecular-weight compounds, and their dependence on temperature confirms the fast water exchange regime.[2,4,5] The results of the simultaneous least-squares fits of the ^{17}O data and the ^{1}H NMRD profiles are summarized for both Gd^{III} complexes in Table 2 and compared to the data reported for chemically related Gd^{III} complexes of DOTA, DO3A-CE, and DO3A-HP (Chart 1). The Gd^{III} complex of DO3A-CE contains one six-membered chelate ring similar to the complexes of $H_3\mathbf{L^1}$ and $H_4\mathbf{L^2}$. The complexes of DO3A-HP and $H_3\mathbf{L^1}$ are noncharged.

The most remarkable results in Table 2 are undoubtedly the values of the water residence times, τ_M. These are almost identical for [$Gd(H_2O)(\mathbf{L^1})$] (39 ns) and [$Gd(H_2O)(\mathbf{L^2})$]$^-$ (34 ns) but approximately 7 times shorter than that for the

$[Gd(H_2O)(dota)]^-$ complex (244 ns).[42] In fact, the values fall near to the optimum for low imaging field (0.5 T) applications, which is in the range 10−30 ns.[1] Thus, the replacement of one of the acetate pendant arms in the structure of DOTA with a pyridine-*N*-oxide arm leads to an acceleration of the water exchange on the Gd^{III} complex. This can have several structural reasons: (i) The six-membered chelate ring formed after coordination of the pyridine-*N*-oxide to the central ion produces an additional steric strain at the water binding site, which facilitates the dissociatively induced water exchange. (ii) Compared to structures of the Ln^{III} complexes of DOTA, the pyridine-*N*-oxide arm slightly increases the distances between N_4 and O_4 planes as found in crystal structures of Ln^{III} complexes of $H_3\mathbf{L^1}$.[39] A correlation between increased N_4-O_4 distances and an accelerated water exchange rate has been suggested.[45] (iii) The newly observed *syn/anti* isomerism of the six-membered chelate ring described in an accompanying paper may also be involved in the water exchange process.[39] Fast water exchange is usually observed on complexes with negative charge[46] and/or with a high content of the twisted-square-antiprismatic isomer.[47,48] However, in our case, the charge of the trivalent Ln ion is compensated for with the three acetate pendant arms and the complex is neutral (for $H_3\mathbf{L^1}$). Moreover, the complexes of $H_3\mathbf{L^1}$ and $H_4\mathbf{L^2}$ were found to exist in a square-antiprismatic (SA) arrangement,[18,39] which generally exchanges water molecules slowly.[47,48] An enlargement of one of the chelate rings thus seems to be a very useful method for the shortening of τ_M, working regardless of the charge and isomerism of the complex. Despite the favorable τ_M values, the ^1H NMR longitudinal relaxivities determined at 310 K and 20 MHz (4.04 mM^{-1} s^{-1} for $[Gd(H_2O)(\mathbf{L^1})]$ and 4.54 mM^{-1} s^{-1} for $[Gd(H_2O)(\mathbf{L^2})]^-$) are only slightly higher than the relaxivity of $[Gd(H_2O)(dota)]^-$ (3.5 mM^{-1} s^{-1}).[44] The reason for this lies in the fast molecular motion characterized by low values of τ_R (see Table 2). Fast molecular motion is a well-known major factor limiting the relaxivity of low-molecular-weight CAs.[1] However, the relaxivity should rise significantly if τ_R is increased, for example, by conjugation of $[Gd(H_2O)(\mathbf{L^2})]^-$ to a macromolecule. In fact, the slightly enhanced relaxivity of the bifunctional derivative may be reflecting the higher determined rotation correlation time (τ_R = 93 ps) in contrast to $[Gd(H_2O)(\mathbf{L^1})]$ (τ_R = 74 ps). The presence of the extra carboxylic group in $H_4\mathbf{L^2}$ and its solvatation can account for such an observation but the differences are too small to give a clear answer. Among the other parameters in Table 2, the values of the zero-field splitting energy (Δ^2) are noticeably higher for the pyridine-*N*-oxide derivatives compared to that of the $[Gd(H_2O)(dota)]^-$ complex. This corresponds well to the lower symmetry of the complexes studied, which was also suggested from the emission spectra of the Eu^{III} complexes.

To the best of our knowledge, there is only one report in the literature describing a Gd^{III} complex of a macrocyclic ligand containing a six-membered chelate ring formed by coordination of a pendant arm, where the relaxometric parameters were given.[8] This complex, $[Gd(H_2O)(do3a\text{-}ce)]^-$ (Chart 1), shows even shorter water residence time than the compounds studied in this paper; other parameters are very similar (Table 2).

Conclusion

The replacement of one of the acetate pendant arms in DOTA with a pyridine-*N*-oxide group radically changed some properties of the Ln^{III} complexes. The complexes are noncharged and possess one water molecule in the first coordination sphere, which exchanges with the bulk with an almost optimal rate. Modification of the pyridine-*N*-oxide with a carboxylic group opens the possibility for attachment of the chelates to macromolecules through an amide bond. The optimal water exchange and short and rigid linkage to macromolecules should ensure a high relaxivity of such conjugates, which are currently being developed in our group. The thermodynamic and kinetic stabilities of the complexes studied are similar to those of the complexes of DOTA[49] and thus fulfill the criteria for applicability in view of the recently discovered toxicity problems.[50]

Acknowledgment. Support from the Grant Agency of the Czech Republic (Grant 203/06/0467), Grant Agency of the Academy of Science of the Czech Republic (Grant KAN2011-10651), and the Long-Term Research Plan of the Ministry of Education of the Czech Republic (Grant MSM0021620857) is acknowledged. The work was carried out in the frame of COST D38 and the EU-supported NoE projects EMIL (Grant LSHC-2004-503569) and DiMI (Grant LSHB-2005-512146).

Supporting Information Available: Experimental data and a detailed description of the structures of $\mathbf{8}\cdot HCl$ and $H_3\mathbf{L^1}\cdot HBr\cdot 0.5NaBr\cdot 11.25H_2O$ and relevant figures; parameters of hydrogen-bond systems found in the structures of $\mathbf{8}\cdot HCl$, $H_3\mathbf{L^1}\cdot 2HCl\cdot 4H_2O$, $H_4\mathbf{L^2}\cdot 2HCl\cdot 2H_2O$, and $H_3\mathbf{L^1}\cdot HBr\cdot 0.5NaBr\cdot 11.25H_2O$; geometry around the Na^I ion found in the structure of $H_3\mathbf{L^1}\cdot HBr\cdot 0.5NaBr\cdot 11.25H_2O$; excitation and emission spectra of $[Eu(H_2O)(\mathbf{L^2})]^-$; variable-temperature ^{17}O T_1 and ^{17}O NMR chemical shift data of $[Gd(H_2O)(\mathbf{L^1})]$ and $[Gd(H_2O)(\mathbf{L^2})]^-$; MS and HPLC characterization of prepared complexes; and the set of equations used for data fitting. This material is available free of charge via the Internet at http://pubs.acs.org.

IC801596V

(44) Laurent, S.; Vander Elst, L.; Muller, R. N. *Contrast Media Mol. Imaging* **2006**, *1*, 128–137.
(45) Kotek, J.; Rudovský, J.; Hermann, P.; Lukeš, I. *Inorg. Chem.* **2006**, *45*, 3097–3102.
(46) (a) André, J. P.; Maecke, H. R.; Tóth, É.; Merbach, A. E. *J. Biol. Inorg. Chem.* **1999**, *4*, 341–347. (b) Zhang, S.; Jiang, X.; Sherry, A. D. *Helv. Chim. Acta* **2005**, *88*, 923–935.
(47) (a) Dunand, F. A.; Dickins, R. S.; Parker, D.; Merbach, A. E. *Chem.—Eur. J.* **2001**, *7*, 5160–5167. (b) Dunand, F. A.; Aime, S.; Merbach, A. E. *J. Am. Chem. Soc.* **2000**, *122*, 1506–1512. (c) Aime, S.; Barge, A.; Botta, M.; De Sousa, A. S.; Parker, D. *Angew. Chem., Int. Ed.* **1998**, *37*, 2673–2675.
(48) (a) Woods, M.; Kovacs, Z.; Zhang, S. R.; Sherry, A. D. *Angew. Chem., Int. Ed.* **2003**, *42*, 5889–5892. (b) Woods, M.; Botta, M.; Avedano, S.; Wang, J.; Sherry, A. D. *Dalton Trans.* **2005**, 3829–3837.
(49) Lubal, P.; Vaněk, J.; Ševčíková, R.; Ševčík, R.; Huserová, J.; Polášek, M.; Hermann, P.; Kotek, J.; Lukeš, I. Unpublished results.
(50) Marckmann, P.; Skov, L.; Rossen, K.; Dupont, A.; Damholt, M. B.; Heaf, J. G.; Thomsen, H. S. *J. Am. Soc. Nephrol.* **2006**, *17*, 2359–2362.